Journal of Magnetism and Magnetic Materials 242–245 (2002) 457–460
journal of magnetism and magnetic materials
www.elsevier.com/locate/jmmm

Local resonant conductance in magnetic tunnel junctions

D. Kechrakos[a,*], E.Y. Tsymbal[b], D.G. Pettifor[b]

[a] Institute of Materials Science, NCSR "Demokritos", 153 10 Athens, Greece
[b] Department of Materials, University of Oxford, Parks Road, Oxford OX1 3PH, UK

Abstract

Using a simple tight-binding model and the Kubo formula we have calculated the lateral distribution of the tunneling conductance across a magnetic tunnel junction probed by scanning tunneling microscopy. We find that the presence of an impurity within the barrier layer can cause a sharp spike in the conductance distribution, in agreement with recent experiments. © 2002 Elsevier Science B.V. All rights reserved.

Keywords: Magnetic tunnel junctions; Impurities; Resonant tunneling; Tight-binding calculation

Magnetic tunnel junctions (MTJs) composed of an insulating layer sandwiched between two ferromagnetic metallic layers exhibit a large tunneling magnetoresistance (TMR), namely a change of their electric resistance under application of an external magnetic field that alters the relative alignment of the magnetizations of the ferromagnetic layers. This effect was first observed in Fe/Ge/Co trilayers at low temperature [1], but recent advances in MTJ preparation demonstrated high TMR values at room temperature [2,3]. These observations generated a lot of interest in these structures also in relation to their potential applications in magnetic sensors and memories [4,5].

In most junctions an alumina barrier is used which is amorphous. The random structure of the barrier makes reproducibility of TMR characteristics harder and the intrinsic mechanism of electron transport much more intricate [6]. MTJs with crystalline insulating barriers offer an appealing alternative. Besides, they make the first-principles studies feasible [7–9]. Recently, Wulfhekel et al. [10] have grown epitaxial single-crystal Fe/MgO/Fe MTJs and measured the lateral distribution of the tunneling current using scanning tunneling microscopy (STM). Interestingly, they observed spikes in the current distribution that attributed to ballistic electrons tunneling via localized impurity states in the MgO barrier.

In this work, we present a simple theoretical model for a MTJ containing an isolated impurity in the barrier layer and coupled to the STM tip [11]. We use a tight-binding description of the electronic structure of the magnetic tunnel junction and the Kubo formula to evaluate the conductance. We demonstrate that resonance tunneling via the impurity state, which is probed by STM, results in a sharp spike in the conductance distribution, in agreement with the experiments of Wulfhekel et al. [10].

The MTJ consists of a semi-infinite metal electrode, an insulating barrier layer and a top metal layer. The current flows across the junction and passes to the metal tip of the STM through a vacuum layer. The tip is modeled by a semi-infinite monatomic wire. The thickness of the barrier, metal and vacuum layers are denoted by L_b, L_m, and L_v, respectively. A single-band tight binding Hamiltonian with nearest neighbor hoppings β and a simple cubic lattice with lattice parameter a is used within this model. On-site atomic energies of the electrode, barrier, metal layer, and tip are denoted by E_e, E_b, E_m, and E_t, respectively. The vacuum is represented by a few atomic monolayers with a potential energy E_v that is high enough to provide no states at the Fermi level. The conductance of the coupled MTJ–tip system is obtained by the Kubo formula [12], according

*Corresponding author. Tel.: +301-6503-313; fax: +301-6519-430.
E-mail address: dkehrakos@ims.demokritos.gr (D. Kechrakos).

PII: S0304-8853(01)01070-8

to which the zero temperature conductance per spin is equal to

$$\Gamma = \frac{2\hbar}{\pi a^2}\mathrm{Tr}[J\,\mathrm{Im}(G)J\,\mathrm{Im}(G)], \quad (1)$$

where G is the Green function of the total coupled system that includes the MTJ with the impurity and the tip. The current operator J can be calculated across the bond between the edge atom of the tip $|t\rangle$ and the adjacent site of the vacuum layer $|v\rangle$. Then J reads

$$J = \frac{ea}{i\hbar}\beta\{|v\rangle\langle t| - |t\rangle\langle v|\}. \quad (2)$$

The Green function G is obtained as follows. First, the Green function of the barrier–metal–vacuum trilayer *without the impurity* is obtained in the **k**-representation, where $\mathbf{k} = (k_x, k_y)$ is the electron transverse wavevector:

$$g^0(\mathbf{k}) = [E_F - H(\mathbf{k}) - \Sigma(\mathbf{k})]^{-1}. \quad (3)$$

Here $H(\mathbf{k})$ is the Hamiltonian of the trilayer and $\Sigma(\mathbf{k})$ is the self-energy correction that arises due to the coupling of the first barrier layer to the surface layer of the electrode. All quantities in Eq. (3) are $L \times L$ matrices, where $L = L_b + L_m + L_v$ is the trilayer thickness. The presence of the impurity perturbs the Green function of the perfect MTJ and application of Dyson equation provides

$$g_{vv} = g^0_{vv} + g^0_{vi}\frac{(E_i - E_b)}{1 - g^0_{ii}(E_i - E_b)}g^0_{iv}, \quad (4)$$

where $g^0(g)$ is the real-space Green functions in the absence (presence) of impurity, v denotes the site in the vacuum layer bonded to the tip and i denotes the impurity site. The Green function elements entering Eq. (4) are obtained by a two-dimensional Fourier transformation of the corresponding **k**-space elements in Eq. (3). Finally, the tip is attached to the top vacuum layer and the relevant matrix elements of the total Green function read $G_{vv} = (g^{-1}_{vv} - \beta^2 g^t)^{-1}$, $G_{vt} = G_{vv}\beta g^t$ and $G_{tt} = g^t(1 + \beta G_{vt})$, where g^t is the Green function on the edge atom of the uncoupled tip.

Fig. 1a shows the calculated variation of the local conductance versus the impurity energy. The tip in this case is located above the impurity site. A pronounced resonance is observed around $E_i/\beta = 1.46$. The asymmetric character of the resonance is a consequence of the Fano effect and stems from the interference between direct and resonant tunneling processes. Further analysis of this effect is presented elsewhere [11]. Furthermore, we show in Fig. 1b the lateral distribution of the conductance as the tip scans the area above the metal film. The impurity energy is chosen at the resonance value ($E_i/\beta = 1.46$). As is seen from Fig. 1b, a pronounced spike of about $10a$ in diameter is observed around the impurity site at $x = y = 0$. We also find that a spike with very similar height and width is observed if

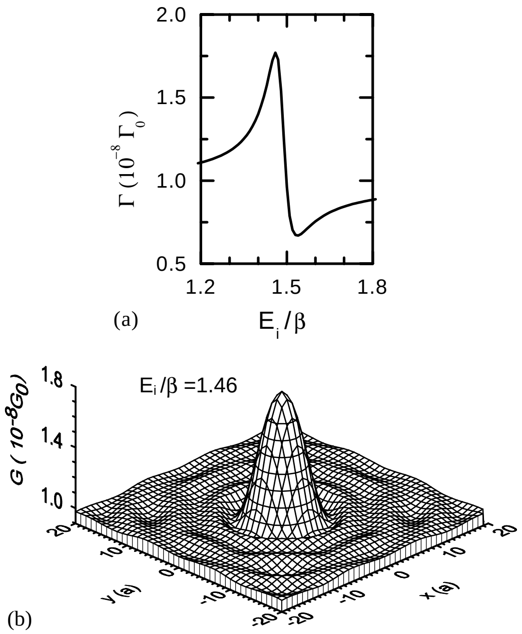

Fig. 1. Junction at zero bias voltage. (a) Dependence of local conductance on the energy level of the impurity, when the tip is located above the impurity site. (b) Lateral variation of the conductance. Parameters used: $E_F = E_t = 0\ E_e/\beta = E_m/\beta = 3.0$, $E_b/\beta = 6.2$, $E_v/\beta = 6.4$, $L_b = 5a$, $L_m = L_v = 10a$.

the tip is placed directly above the barrier layer, that is, before the top metal film is grown (not shown).

A physical picture for the emergence of this spike is as follows. Consider electrons traveling ballistically from the electrode towards the tip, with a momentum along the tip axis. The impurity acts as a strong scattering center that changes isotropically the direction of the electron momentum. The vacuum layer acts as a filter for the electrons that emerge from the impurity with a substantial transverse momentum. This layer selects only electrons with minute transverse momenta passing into the tip that give rise to a spike in the conductance above the impurity site. Both our results for the metal-insulator and the metal–insulator–metal systems give full support to the interpretation of the spikes in the STM measurements of Wulfhekel et al. [10] as due to impurity-mediated resonant tunneling.

Our model does not predict, however, any spike in the conductance map if the tip is placed in contact with the top metal film. The absence of the vacuum layer between the tip and the top metal film prevents electrons from filtering in a narrow angular window close to normal incidence and, therefore, allows detecting electrons that tunnel at *any* lateral position. In this case the dominant contribution comes from *non-resonant* tunneling and the conductance is weakly dependent on the tip position. This result is in contrast to the experiments [10], where

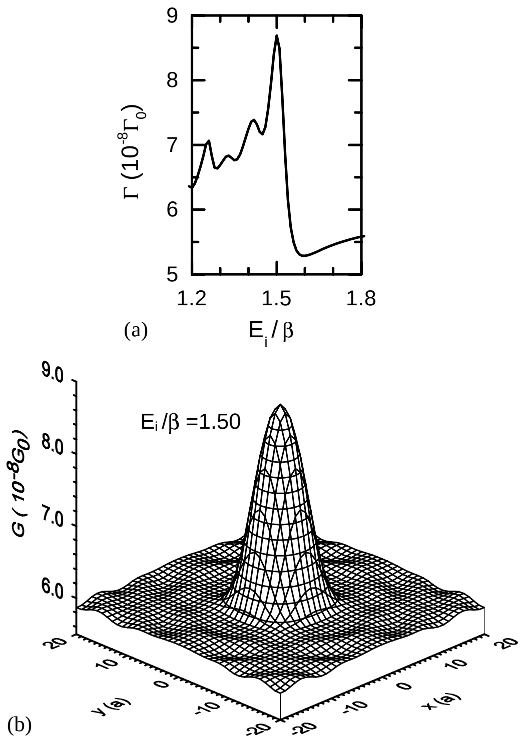

Fig. 2. Same as in Fig. 1 for a bias voltage $V/\beta = -0.5$.

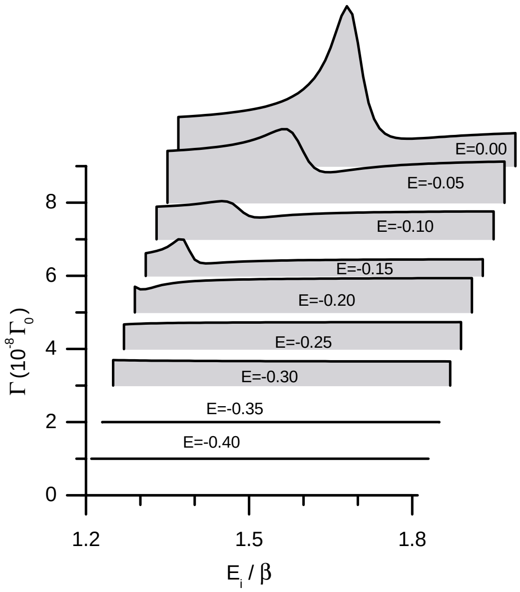

Fig. 3. Contributions to local conductance from electrons with different energies in the range (E_F, $E_F + V$). Parameters used: the same as in Fig. 2.

spikes in the conductance were observed using an AFM in a contact mode. Since a true metallic contact does not allow detecting a localized state within the barrier, we anticipate that features of the contact itself are responsible for the spikes in these experiments.

When a bias voltage V is applied across the MTJ this is shared between the insulating layer and the vacuum layer. To a first approximation, we neglect space charge effects in the insulator and the image potential in the vacuum layer and assume a linear decrease of the electric potential both inside the barrier and the vacuum. Then, the zero-temperature conductance of the biased junction reads

$$\Gamma(V) = \int_{E_F}^{E_F+V} \Gamma(E)\,\mathrm{d}E, \tag{5}$$

where $\Gamma(E)$ is obtained from Eq. (1) with the appropriate potential profile in the Hamiltonian entering Eq. (3). As is seen from Figs. 2a and b, bias leads to increase in conductance and reduction in contrast between the high and low conductance values, but the spike is still clearly observed. Under bias all electrons with energies in the range $(E_F, E_F + V)$ contribute to the ballistic transport across the MTJ. The contribution to the total conductance from electrons with different energies is plotted in Fig. 3. Electrons with lower energy suffer stronger attenuation in the vacuum barrier and consequently they contribute less to the conductance, while the resonant character of their conductance is suppressed. A shift of the resonant peak to lower impurity energies is observed as the vacuum barrier felt by the impinging electrons is increased. The partial resonances are present in the integrated conductance (Fig. 2a) and produce a broad shoulder below the main resonance at $E_i/\beta = 1.50$.

In conclusion, we have evaluated the local ballistic conductance probed by STM in a magnetic tunnel junction which contains an isolated impurity within the barrier layer. We found that the resonant character of the tunneling process through the localized state manifests itself in a conductance spike above the impurity site, which is preserved under applied bias. We believe that these results will stimulate using STM to elucidate the nature of defects in magnetic tunnel junctions and to study their influence on local TMR.

References

[1] M. Julliere, Phys. Lett. A 54 (1975) 225.
[2] J.S. Moodera, L.R. Kinder, T.M. Wong, R. Meservey, Phys. Rev. Lett. 74 (1995) 3273.
[3] T. Miyazaki, N. Tezuka, J. Magn. Magn. Mater. 139 (1995) L231.
[4] P.M. Levy, S. Zhang, Curr. Opin. Solid State Mater. Sci. 4 (1999) 223.
[5] J.S. Moodera, J. Nassar, G. Mathon, Ann. Rev. Mater. Sci. 29 (1999) 381.

[6] E.Y. Tsymbal, D.G. Pettifor, Phys. Rev. B 58 (1998) 432.
[7] I.I. Oleinik, E.Y. Tsymbal, D.G. Pettifor, Phys. Rev. B 62 (2000) 3952.
[8] Ph. Mavropoulos, N. Papanikolaou, P.H. Dederichs, Phys. Rev. Lett. 85 (2000) 1088.
[9] W.H. Butler, X.G. Zhang, T.C. Schultless, J.M. MacLaren, Phys. Rev. B 63 (2001) 54416.
[10] W. Wulfhekel, M. Klaua, D. Ullmann, F. Zavaliche, J. Kirschner, R. Urban, T. Monchesky, B. Heinrich, Appl. Phys. Lett. 78 (2001) 509.
[11] E.Y. Tsymbal, D.G. Pettifor, Phys. Rev. B 64 (2001) 212401.
[12] P.A. Lee, D.S. Fisher, Phys. Rev. Lett. 47 (1981) 882.